Journal of Power Sources 193 (2009) 547–554

Contents lists available at ScienceDirect

Journal of Power Sources

journal homepage: www.elsevier.com/locate/jpowsour

A performance and degradation study of Nafion 212 membrane for proton exchange membrane fuel cells

Adriano C. Fernandes, Edson Antonio Ticianelli*

Instituto de Química de São Carlos, Universidade de São Paulo, Av. Trabalhador SaoCarlense, 400, CP 780, 13560-970 São Carlos-SP, Brazil

ARTICLE INFO

Article history:
Received 9 March 2009
Received in revised form 17 April 2009
Accepted 20 April 2009
Available online 3 May 2009

Keywords:
PEM fuel cell
Nafion 112
Nafion 212
Nafion degradation

ABSTRACT

The operational characteristics of the Nafion® 212 membrane (N212) are investigated and compared to that of Nafion® 112 (N112), in proton exchange membrane fuel cells (PEMFCs). The consequences of the membranes' degradation are also investigated, after accelerated aging experiments using Fenton's method. Studies were performed by single cell polarization and impedance measurements, as a function of the cell and gas humidification temperatures and the gases pressures. Polarization curves show that the cell with N212 presents higher performance than that with N112, when operating under air cathode. FTIR analyses indicated that the chemical structure of Nafion does not change after accelerated degradation tests for both membranes. In spite of this, significant differences were observed in the morphology, mainly for N212. The electrochemical studies confirmed that the degradation of the membranes leads to a reduction of the fuel cell performance by increasing the gas crossover, mainly H_2. Results also show that the N212 membrane may be less durable than N112.

1. Introduction

Proton exchange membrane fuel cells (PEMFCs) have gained worldwide attention as a successful device to replace combustion engines, mainly because of their higher performance and low pollutant emissions. Despite the large technological developments of PEMFCs in the last decade, there is still a need to increase its performance, in other words, higher stability and reduced costs [1–7].

The electrolyte membrane is one of the most important parts of the PEMFC membrane and electrode assembly (MEA). It works the MEA's ionic conductor, gas barrier and mechanical support. One of the problems of the polymer electrolyte membrane has been the water management, as the performance and durability of this component depend on the water balance [8–19]. If the membrane is not appropriately hydrated, it shows a high ionic resistance and it can be irreversibly damaged, therefore any excess water has to be removed to avoid the electrode flooding. The hydration state of the membrane is strongly affected by inside water transport, which is dominated by three mechanisms, namely, electro-osmotic drag, convection and back diffusion/convection. The former is caused by proton migration from the anode to the cathode. The second is due to gas pressure gradients in the fuel cell, while the latter is due to the existence of water concentration gradients between the cathode and the anode [8]. When the amount of liquid water is high, it blocks the pores of the catalyst layer of the electrode, preventing the flow of gases and restricting access of the reactants to the catalyst sites.

Parameters such as pressure, humidification, and temperature have a decisive influence on the performance of PEMFCs. Sethuraman et al. [20] showed that gas humidity affects the mechanical durability of the membranes, mainly when the fuel cell operation is in frequent start–stop cycles, because frequent wet-up and dry-out cycles cause mechanical stress to the membrane. Paganin et al. [21] demonstrated that high temperatures cause severe loss of water by evaporation. They showed that the optimum temperature for a good performance of PEMFCs is 80 °C for the cell, and 85 °C and 95 °C for the oxygen and hydrogen humidifiers, respectively.

A key factor to achieve a long working lifetime is to improve the durability of the ionomer both in the membrane and in the electrode catalyst layer, in order to avoid gas crossover and prevent the reduction of the ionic conductivity and the loss of mechanical stability of the membrane electrode assembly. Several membrane degradation modes have been observed, as for example, mechanical or thermal stress and chemical or electrochemical degradation [22–30]. Studies have shown that chemical degradation of the polymer electrolyte occurs during the fuel cell operation, caused by the attack of radical species (hydroxyl and peroxyl) formed in the MEA as reaction intermediates, particularly in the oxygen reduction reaction (ORR). It has also been suggested that the metal ions released from the metallic components, as bipolar plates or humidification bottles, can raise the decay rate of the proton exchange membrane [26,29,31,32].

* Corresponding author. Tel.: +55 16 33739945; fax: +55 16 33739952.
E-mail address: edsont@iqsc.usp.br (E.A. Ticianelli).

0378-7753/$ – see front matter © 2009 Elsevier B.V. All rights reserved.
doi:10.1016/j.jpowsour.2009.04.038

Accelerated tests have been used to investigate the lifetime of the membrane, by employing the Fenton reaction:

$$H_2O_2 + Fe^{2+} \rightarrow Fe^{3+} + OH\cdot + OH^-$$

to produce OH·, which attacks the membrane fluorinated end groups, for example, $-CF_2COOH$, $-CF_2H$ or $-CF{=}CF_2$:

(i) $R{-}CF_2COOH + OH\cdot \rightarrow R{-}CF_2\cdot + CO_2 + H_2O$

(ii) $R{-}CF_2\cdot + OH\cdot \rightarrow R{-}CF_2OH \rightarrow R{-}COF + HF$

(iii) $R{-}COF + H_2O \rightarrow R{-}COOH + HF$

Kinumoto et al. [26] used Fenton's reaction to investigate the stability of the Nafion 117 membrane. The results showed that both main and side chains are decomposed at similar rates by radical attack. Kundu et al. [28] compared two methods for promoting Fenton's reaction (solution and ion exchange) in order to induce the degradation of Nafion membranes. They found that the two degradation methods cause the same damage to the membrane, losing over 20% of their original weight after the tests.

This paper evaluates the performance and stability of PEM fuel cells with Nafion® 212 membrane by using single cell steady-state polarization, hydrogen crossover and impedance measurements. The stability studies were carried out using Fenton's reaction to promote accelerated membrane degradation. The results are then compared to those obtained with the Nafion® 112 membrane (hereafter called N112), for which some studies can be found in the literature [33,34], in contrast to the case of the Nafion® 212 membrane (hereafter called N212). The electrochemical impedance studies were conducted to characterize the polarization phenomena due to the charge transfer kinetics and the resistive and diffusive effects that reduce the cell performance [35,36].

2. Experimental

2.1. Membrane and electrode assembly (MEA) preparation

The gas diffusion electrodes were fabricated according to a well-developed method used in our lab [36]. A standard electrode (cathode and anode), with an active area of 4.62 cm^2, was prepared with 20 wt.% Pt/C, 0.4 mg Pt cm^{-2} and 1.1 mg Nafion® cm^{-2} in the catalyst layer. Electrodes with Nafion® loadings in the range of 1.1–2.2 mg Nafion® cm^{-2} were also prepared. The single cells were built with both types of Nafion® membranes, N212 and N112, both of the same thickness (50 μm).

The membrane electrodes were first assembled by placing a piece of the Nafion® membrane between two electrodes, which were next hot-pressed at 125 °C and 50 atm for 2 min. Different types of single cells were mounted using N112 and N212 with a standard electrode at the anode and with the cathodes containing distinct Nafion loadings.

2.2. Electrochemical tests in single cells

Polarization curves were obtained in a test station, for single-cells feed with H_2 and air/O_2 at several pressures and temperatures. Linear sweep voltammetric measurements were carried out to verify the hydrogen crossover through the membrane. For these experiments, the cell was fed with argon at the cathode side and hydrogen at the anode/reference side. The amount of hydrogen crossing the membrane was comparatively measured by the current intensity of the of linear sweep voltammetric anodic scan.

The impedance measurements were carried out in galvanostatic mode using a frequency response analyzer (FRA) coupled to the test station. The frequency range was from 100 mHz to 10 kHz, covered with 10 points $decade^{-1}$. The impedance spectra were recorded for different current densities, in the range of 0.10–1.90 mA cm^{-2}.

2.3. Procedures for Nafion membrane degradation

Deteriorated Nafion membranes were obtained by the ion exchange method [26,28]. Samples of Nafion were soaked in 0.1 mol dm^{-3} $FeCl_2{\cdot}4H_2O$ (reagent grade) for 24 h. The samples were then rinsed with highly purified water for at least 1 h. Next, they were left in vials to which 40 mL of a 30% hydrogen peroxide solution was added, for 24 h or 48 h at a temperature of 72 °C. After these times, the samples were removed from the solution, rinsed with hot pure water and then conditioned in 1 M H_2SO_4 to remove any residual iron and then the membrane was returned into the H^+ form.

2.4. Fourier transform infrared spectroscopy (FTIR)

Samples of fresh and degraded Nafion membranes (N212 and N112) were chemically analyzed by FTIR, in a Bomem—MB-102 equipment. The spectra were measured using an ATR device (Gateway™). The spectrum was collected after 64 scans both for the background and the sample, with a wave number resolution of 4 cm^{-1}, in the range of 4000–650 cm^{-1}. Background subtraction was used and measurements were carried out at room temperature.

2.5. Scanning electron microscopy (SEM)

Scanning electron microscopy was employed to analyze the membrane morphological structure. The images were obtained using a LEO SEM (model 440) equipment. Samples were covered with a 10 nm layer of Au using a BAL-TEC MED 020 coating system to improve conductivity.

3. Results and discussion

Information about the electrolyte resistance and the kinetic parameters of the oxygen reduction reaction was obtained for the different single cell systems by analyzing the experimental polarization data using the semi-empirical equation [37,38]:

$$E = E^0 - b \log i - Ri \quad (1)$$

where $E^0 = E_r + b \log i_o$, E_r is the reversible potential of the cell, b is the Tafel slope and i_o is the exchange current density for the oxygen reduction reaction in the catalyst. R represents the total contribution of linear polarization components, which include the charge transfer resistance of the hydrogen oxidation reaction, the ionic resistance of the electrolyte in the cell (inside the catalyst layer and inside the membrane), the electronic resistance and the linear diffusion terms related to limitations by the diffusion of the reactant gases [38]. In the range of the current density used in the fits, it can be assumed that the electrolyte resistance is independent of the current density [37]. Eq. (1) does not include limitations from diffusion, except for linear contributions and because a change on the Tafel slope is expected at around 0.8 V (oxygen electrode potential) [39], this analysis only considered the data of cell potentials above this value.

3.1. Effects of the cell and humidifiers temperature

Fig. 1 shows the effect of the temperature on the steady-state polarization curve obtained for single cells with N212 and N112 membranes, working with H_2/air at 2:3 atm, and keeping the gases humidification and the cell at the same temperature. Typical profiles already reported for PEMFC with Nafion membranes [21,40]

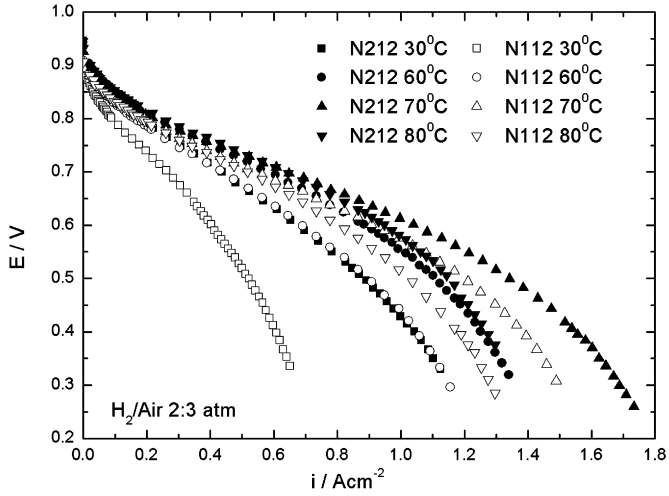

Fig. 1. Steady state polarization curves for single cells at several temperatures with N212 (full symbol) and N112 (open symbol) membranes, H_2 (2.0 atm) and air (3.0 atm) as anode and cathode feed. $T_{H2} = T_{Cell} = T_{Air}$.

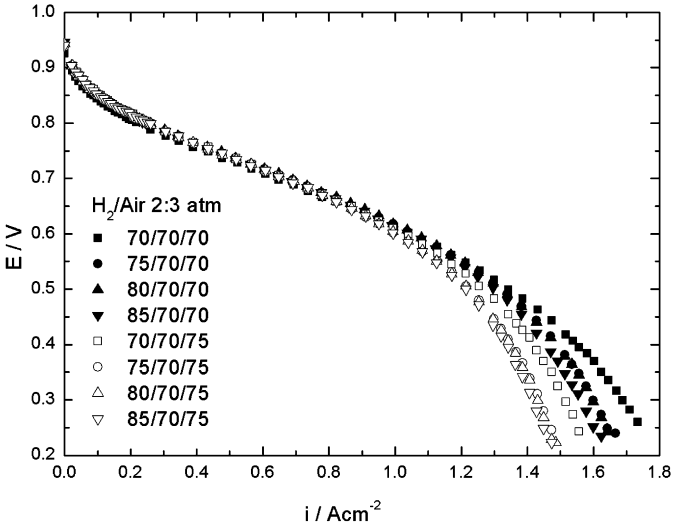

Fig. 2. Steady state polarization curves for single cells with N212 membrane operating with H_2 and air, for several gas humidification temperatures.

are observed for the cell with the two different membranes. An increase of the limiting current with temperature is observed up to 70 °C, after which the performance decreases. It is also noteworthy that the N212 membrane shows a better performance than N112 for all temperatures.

Table 1 shows the kinetic parameters (E^0, b, and R) resulting from the fitting of Eq. (1) to the experimental polarization results in Fig. 1. These data denotes higher values of E^0 and smaller values of R for the system with N212, at all temperatures, thus indicating less crossover of gases and higher membrane conductivity for N212. On the other hand, the increase of E^0 and the reduction of R for both membranes with the temperature increase are consequences of the improved reaction kinetics and membrane conductivity, as already reported [38,41]. As expected, the Tafel slope values resulted close to 60/70 mV dec^{-1}, in agreement with many other results obtained for the oxygen reduction on Pt-based catalysts [21,38].

It has been shown that the best humidification conditions for PEMFC with Nafion membranes is that in which the gases and cell operate at different temperatures [37]. In the resent work, in order to obtain the best system operation conditions, experiments were carried out changing the humidification temperatures of the reactant gases, with these results displayed in Fig. 2. The humidification temperatures were changed from 70 °C to 85 °C and 70 °C to 75 °C for hydrogen and air, respectively. In all cases, it is observed that the polarization curves have the same profile until 1 A cm^{-2}, indicating that the reaction kinetics and the membrane resistance are not affected by the humidification conditions. A decrease of the limiting current is observed when the gases temperature is increased by 5 °C or more higher than that of the cell. This effect can be associated with the appearance of diffusion problems due to water condensation, which renders difficult the reactant gases reaching the electrode catalyst sites. The phenomenon is more pronounced for the cathode, indicating that the flooding problems are more serious in the cathode, probably because of water accumulations caused by the crossover and the production *via* oxygen reduction.Identical fitting parameters were obtained for the different humidification temperatures (not shown), as expected for a case where the cell remains at a constant temperature (70 °C).

Table 1
Kinetic parameters (E^0, b, R) obtained from fitting of Eq. (1) to experimental polarization results for single cells with N112 and N212 membranes at different temperature. Values of the OCP (open circuit potential), R_{EIS} (high frequency resistance) and Power (0.7 V) (power density at 0.7 V) are also included. P_{H2} = 2 atm and P_{Air} = 3 atm.

Temperature (°C)	E_{OCP} (mV)	E^0 (mV)	b (mV dec^{-1})	R (Ω cm^2)
Membrane N212				
30	946	799	65	0.27
60	943	811	61	0.21
70	926	794	65	0.16
80	931	811	58	0.18
Membrane N112				
30	895	784	53	0.43
60	909	811	47	0.29
70	907	802	52	0.21
80	907	802	53	0.23

3.2. *Effects of the gases pressure*

The effect of the air pressure on the fuel cell performance for both membranes at the same cell and humidification temperature (70 °C) is shown in Fig. 3. When the cell works with non-pressurized O_2, the performance is almost the same, independently of the membrane. On the other hand, Fig. 3 shows that for all air pressures the cell performances are higher with N212 than those with N112. It is

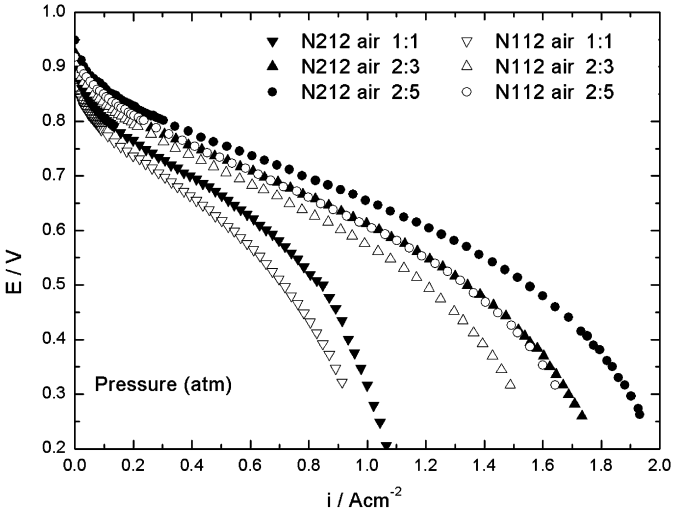

Fig. 3. Steady state polarization curves for single cells with N212 (full symbol) and N112 (open symbol) membranes operating with H_2 and air at different pressures. $T_{H2} = T_{Cell} = T_{Air}$ = 70 °C.

Table 2
Kinetic parameters (E^0, b, R) obtained from fitting of Eq. (1) to the experimental polarization results for single cells with N112 and N212 membranes at different pressures. Values of the OCP (open circuit potential), R_{EIS} (high frequency resistance) and Power (0.7 V) (power density at 0.7 V) are also included. $T_{H2} = T_{Cell} = T_{Air} = 70\,^{\circ}C$.

Pressure, H_2/air (atm)	E_{OCP} (mV)	E^0 (mV)	b (mV dec^{-1})	R (Ω cm^2)	R_{EIS} (Ω cm^2)	Power (0.7 V) (W cm^{-2})
Membrane N112						
2:5	918	811	57	0.19	0.19	0.44
2:3	907	802	52	0.21	0.19	0.39
1:1	864	748	57	0.22	0.19	0.21
Membrane N212						
2:5	949	817	59	0.15	0.17	0.54
2:3	926	794	65	0.16	0.17	0.45
1:1	901	766	63	0.22	0.17	0.28

also noted that when the N212 membrane is used, the cell reaches higher limiting current densities and this is probably related to problems of gas diffusion decrease, associated with smaller cathode flooding due to less water electro-osmotic dragging from the anode to the cathode [42]. The power densities ($E \times i$) obtained from the results in Fig. 3 at a cell potential of 0.7 V are included in Table 2. It is noted that the cells built with N212 show an improvement of 23, 16 and 29% in the power density when compared to N112, both operating with H_2/air 2:5, 2:3 and 1:1 atm, respectively.

The kinetic parameters obtained from the fitting of Eq. (1) to the data in Fig. 3 are included in Table 2. It is seen that the increase of pressure causes an increase of the kinetics of the oxygen reduction reaction, as confirmed by the rising of E^0. This might be a consequence of the increase in the electrode reversible potential, and also the increase in the exchange current density due to the gas solubility increase. For both membranes, R decreases with the increase of pressure, and this may be assigned to a higher gas flux to the catalytic sites, leading to a decrease of linear diffusion effects. It is interesting to note that in all cases, the R values for N212 are smaller than those for N112, confirming an improvement in the N212 membrane properties.

The polarization phenomena due to the reaction kinetics and the resistive and diffusive effects were also investigated as a function of pressure by electrochemical impedance spectroscopy. Fig. 4 shows Nyquist impedance plots for the PEMFC at 70 °C, working at several pressures for the reactant gases. The high frequency impedance values that essentially represent the membrane resistance (R_{EIS}) are included in Table 2. It can be observed that the R_{EIS} values of N212 are smaller than those of N112 in all experimental conditions. This decrease in the membrane resistance causes a decrease in the ohmic drops of the fuel cell, which can then reach higher current densities at lower overpotentials.

In general, the impedance plots for both membranes presented the same characteristic features for all applied pressures. At the high frequency region there is an arc with the magnitude independent of the current density; at middle frequencies there is another arc that decreases with the increase of the current density until a given value (0.3 A cm^{-2}, 0.5 A cm^{-2} and 0.7 A cm^{-2} for pressures of 1:1, 2:3 and 2:5 atm, respectively), after which the arc magnitude increases.

These results indicate that there are two phenomena controlling the electrode behavior at the middle frequency region, depending on the current density. Thus, the decrease of the arc magnitude, as clearly seen at the lower current densities, must be related to the decrease of the charge-transfer resistance. When the current densities increase, diffusion limitations start to become more and more relevant until, after a given current density, depending on the

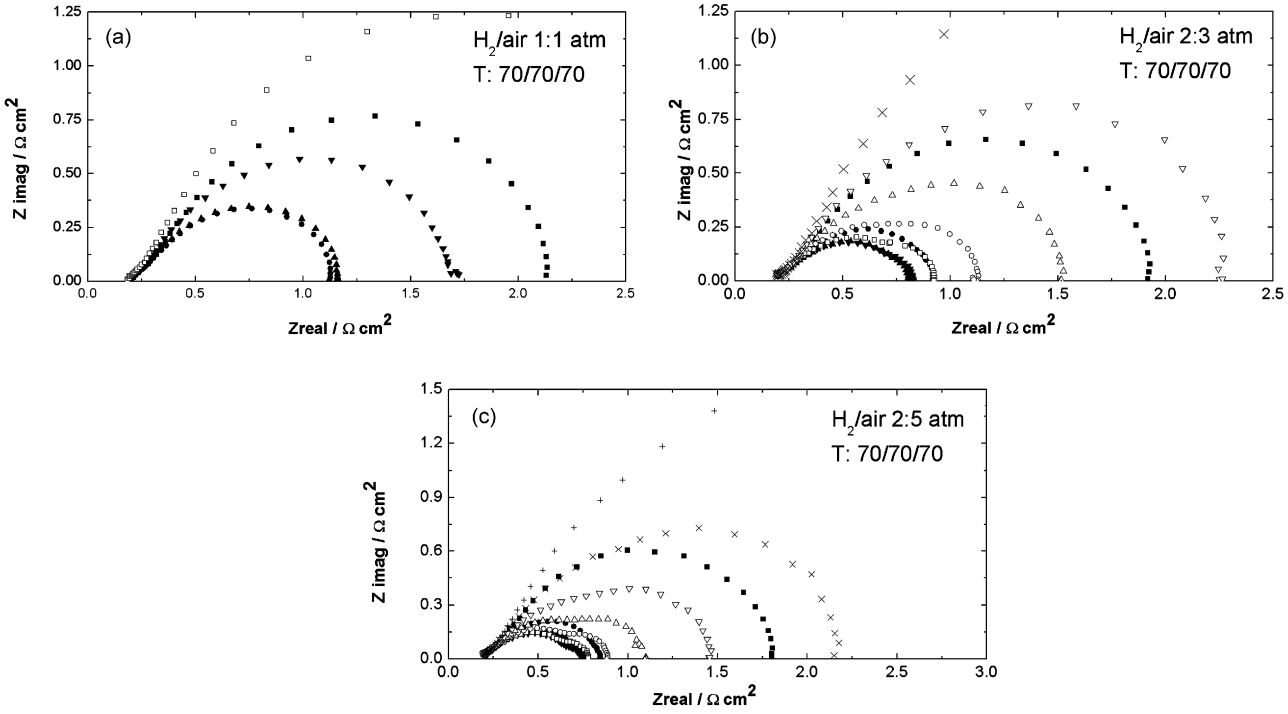

Fig. 4. Impedance plots at several current densities (■ 0.10; ● 0.30; ▲ 0.50; ▼ 0.70; □ 0.90; ○ 1.10; △ 1.30; ▽ 1.50; × 1.70; + 1.90 A cm^{-2}) for single cells with N212 membrane; (a) H_2 (1.0 atm)/air (1.0 atm); (b) (2.0 atm)/air (3.0 atm) and (c) H_2 (2.0 atm)/air (5.0 atm). $T_{H2} = T_{Cell} = T_{Air} = 70\,^{\circ}C$.

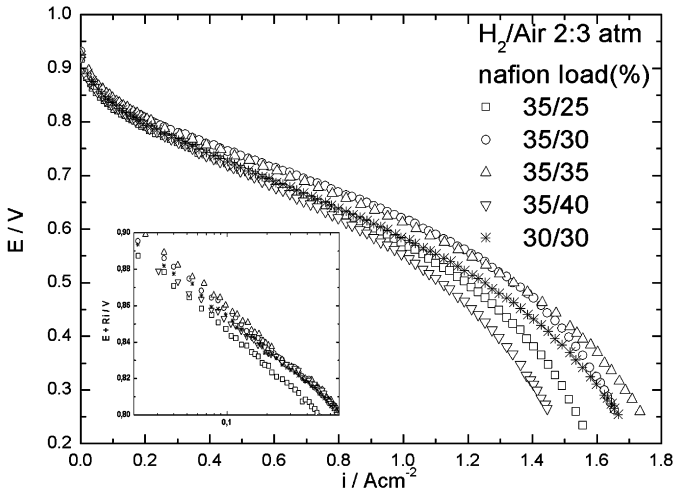

Fig. 5. Steady state polarization curves for single cells with N212 membrane operating with H_2 and air as anode and cathode feed, respectively, for several Nafion loads in the catalyst layer of the cathodes (anodes with 30 or 35%). $T_{H2} = T_{Cell} = T_{Air} = 70\,^{\circ}C$. Insert: Tafel plots for low current densities.

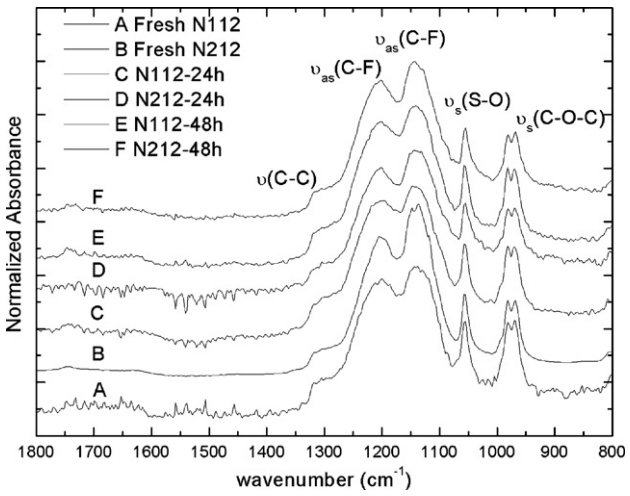

Fig. 6. FTIR spectra of the N212 and N112 Nafion membranes, before (A and B) and after (C–F) the accelerated degradation procedures, for 24 h and 48 h.

pressure, they overcome the charge-transfer effect, consequently the increase of the impedance arc. It is also observed that for a fixed current density there is a reduction of the middle frequency impedance with a pressure increase, and this must be due to an improvement in the kinetics of the oxygen reduction reaction.

3.3. Effects of the Nafion load in the cathode catalyst layer

Fig. 5 depicts the polarization curves of fuel cells with cathodes prepared with Nafion contents of 25, 30, 35 and 40% in the catalyst layer and with N212. Fuel cell performances were evaluated at 70 °C, with H_2/Air at 2/3 atm. The polarization curves indicate cell performance changes with the Nafion load change in the cathode catalyst layer, particularly at high current densities. It can be noted that the electrode performance is poorer both for 25% and 40% of the Nafion contents. Low Nafion contents result in a poor contact between the electrolyte and the catalyst particles, consequently leading to a decrease in the electrode performance caused by the increase in the ohmic effects and the active area decrease [42,43]. In contrast, high Nafion loads in the catalyst layer causes an electrode performance reduction due to the difficulty in the gases reaching the active sites, hence increasing the mass transport overpotentials [42,43]. The Nafion content of 35% represents the best situation, in which a compromise between the two opposite tendencies is reached.

Table 3 shows the kinetic parameters obtained by the fitting of Eq. (1) to the polarization results for the cell with cathodes with different Nafion loads in the catalyst layer. The E^0 values slightly increased with the Nafion load increase, and this must be related to the increase in the Pt active area. A small decrease of R occurred when the Nafion load changed from 25 to 30–35%, and this is consistent with an electrolyte conductivity increase in the catalyst layer. There is a small increase of R when the Nafion load is increased from 35 to 40% and this may be linked to the increase of the diffusion problems.

In summary, it is seen that the fuel cell behavior with N212 follows the same trends as those generally found for Nafion® 112, 115 and 117 [21], although they present different water electro-osmotic and resistivity properties.

3.4. Effects of the membrane degradation

Accelerated degradations of N212 and N112 membranes were promoted by the ion exchange method [26,28], as described above. Fig. 6 shows FTIR spectra of fresh and deteriorated membranes. The peak at 1057 cm^{-1} is due to S–O stretching. The doublet peaks at 968 and 982 cm^{-1} are characteristic peaks of the side chains of Nafion, and are assigned to the symmetric vibrations of C–O–C bonds. The shoulder at around 1300 cm^{-1} is from the C–C bonds. Other peaks [26,28] of interest are at 1144 and 1203 cm^{-1}, which are attributed to anti-symmetric vibration of the C–F bonds of Nafion. The FTIR results showed no significant change after the degradation of the membranes, indicating that the chemical structure of N212 and N112 membranes – the main chains and the side chains – were not substantially decomposed by radical attack. In spite of any evidence of FTIR, the occurrence of a reduction in the average molecular weight as proposed before [26,28], cannot be discarded.

Figs. 7 and 8 represent images of the surface and the cross-section morphologies of N212 (right side) and N112 (left side) membrane samples, before and after accelerated degradation procedures at different times (24 h and 48 h). It is seen that the structure of both fresh membranes are very similar. After degradation, the N112 membrane shows less damage on the surface when compared to N212, either after 24 h or 48 h of OH· exposure. Large defects, such as bubbles, tears and bumps, are found in the N212 membrane surface, while the damage for N112 is far less expressive. Fig. 8b, d, and f shows that the degradation progression for the N112

Table 3
Kinetic parameters (E^0, b, R) obtained from the fitting of Eq. (1) to the experimental polarization results in Fig. 6, for single cell with cathodes with different Nafion loads. Values of the single cell power densities at 0.7 V are also included.

Nafion load (%) anode/cathode	E^0 (mV)	b (mV dec^{-1})	R ($\Omega\,cm^2$)	Power (0.7 V) ($W\,cm^{-2}$)
35/25	782	65	0.18	0.38
35/30	794	63	0.15	0.48
35/35	794	65	0.16	0.45
35/40	798	54	0.21	0.36

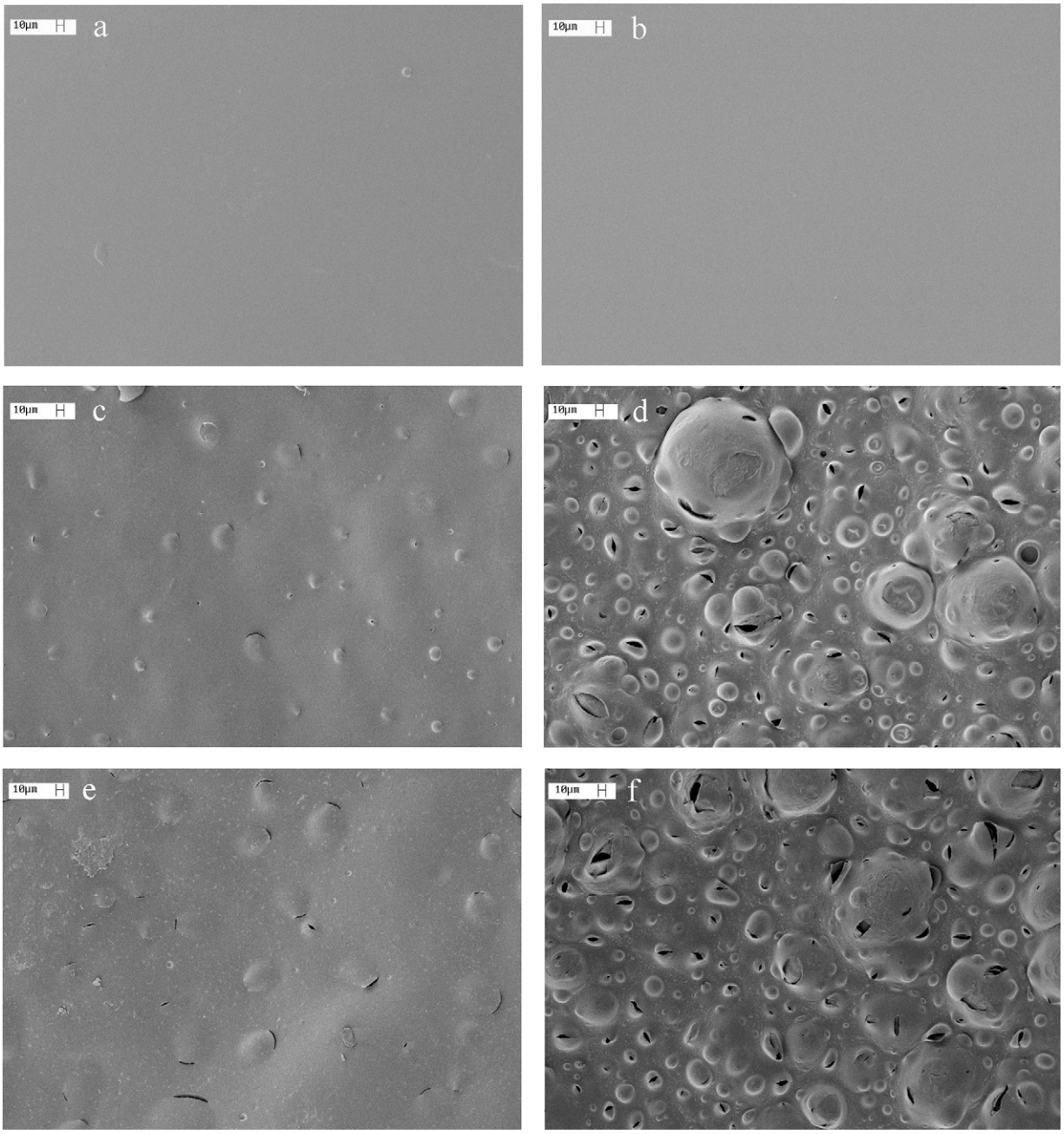

Fig. 7. Scanning electron micrographies of the membrane surfaces (500×): Nafion N112 (a) fresh, after: (c) 24 h and (e) 48 h of degradation; Nafion 212 (b) fresh, after: (d) 24 h and (f) 48 h of degradation.

membrane may lead to a reduction in thickness, while no significant change on the cross-section is seen for N112. Therefore, although the FTIR results do not show chemical differences between the fresh and degraded membranes, scanning electron microscopy analyses indicated significant change in the morphology after the accelerated degradation procedures. In fact, these last results suggest that N212 membrane may be less durable than N112.

Fig. 9 shows the comparison among steady-state polarization curves obtained for single cells with degraded membranes for 24 h and fresh membranes, working with H_2/air 1/1 atm at 70 °C. The polarization curves were recorded at ambient pressures to avoid any risk that could result from the appearance of excessive gas crossover in the degraded membranes. As previously shown (Fig. 3), the MEA built with the N212 membrane, initially presents a higher performance than N112, but after they were submitted to the degradation process, this advantage disappeared (Fig. 9).

From the results in Table 2, it can be noted that the open circuit potentials, E_{OCP}, of the single cells built with fresh N212 membrane are higher than with N112, indicating smaller hydrogen crossover in the former case. After the accelerated degradation procedure the values of E_{OCP} decreased and became almost the same for both degraded membranes (836 mV for N212/24 h and 842 for N112/24 h). This open circuit potential decrease must be related to the hydrogen crossover increase through the membrane.

To confirm this, a hydrogen crossover assessment was made by the electrochemical detection of the molecular hydrogen passing through the membrane, these results are depicted in Fig. 10. It can be seen that the oxidation currents of the hydrogen crossing the membrane are smaller for fresh N212 than for N112, confirm-

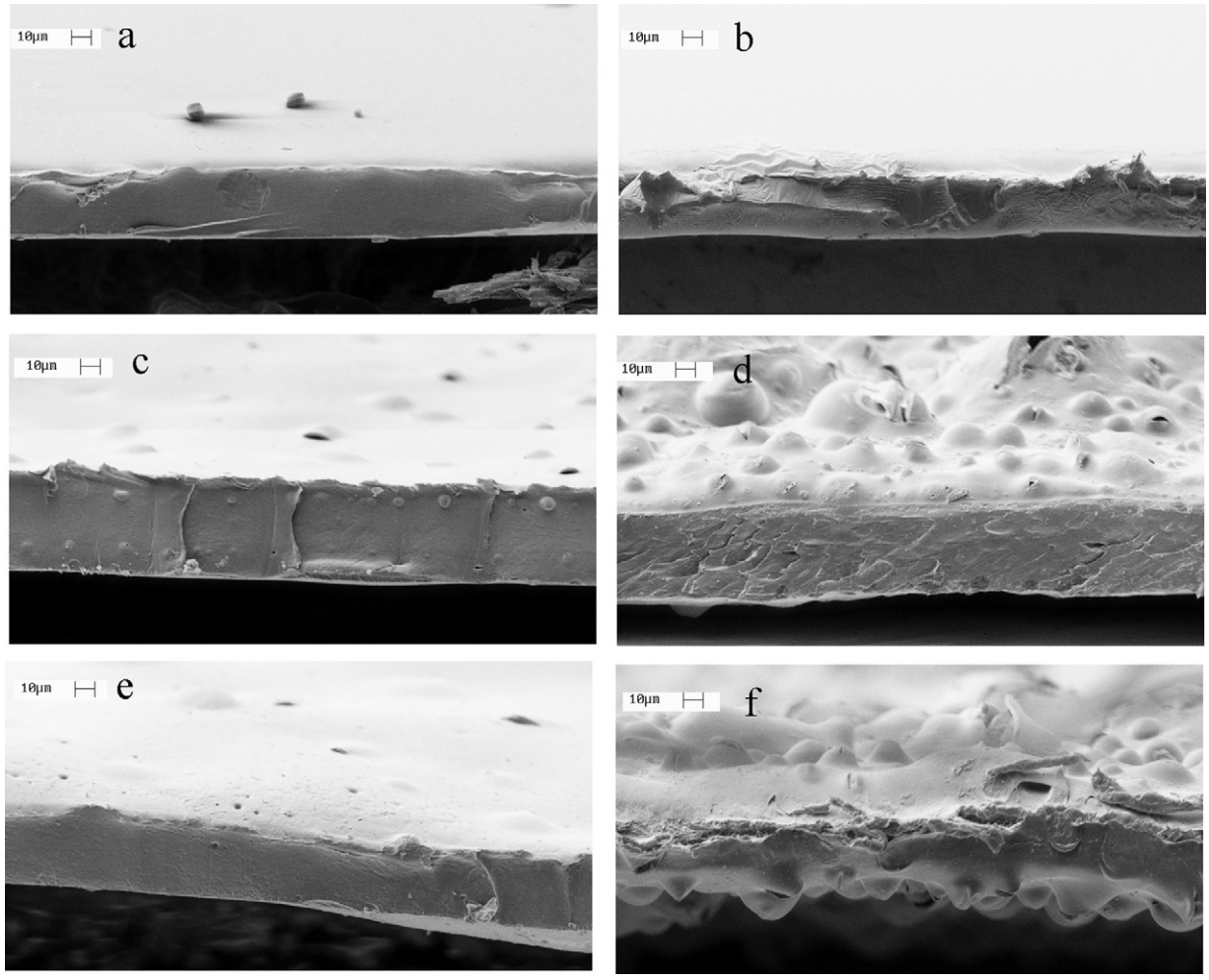

Fig. 8. Scanning electron micrographies of membrane cross-sections (1000×): N112 (a) fresh, (c) after 24 h of degradation and e) after 48 h degradation; N212 (b) fresh, (d) after 24 h and (f) 48 h of degradation.

ing the smaller crossover. At 0.2 V the value obtained for N112 is about 2.4 mA cm^{-2}, while for N212 it is 1 mA cm^{-2}. The value for N112 is consistent with those presented in the literature for Nafion membranes [44–46], which are in the range of 1–2 mA cm^{-2}, depending on the membrane thickness, measurement conditions, and the procedure of preparation of the membrane and electrode assembly. Fig. 10 shows that after the degradation, the hydrogen crossover increased in both cases, but here the hydrogen oxidation currents for N212 membrane were higher than for N112. This demonstrates that in spite of the single cell having initially been

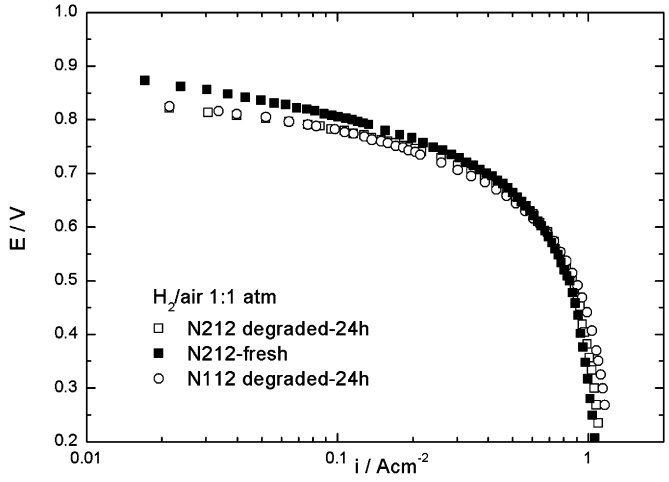

Fig. 9. Steady state polarization curves (logarithm scale) for single cells with N212 before accelerated degradation for 24 h, N212 and N112 after accelerated degradation; H_2 (1.0 atm)/air (1.0 atm). $T_{H2} = T_{Cell} = T_{Air} = 70\,^{\circ}C$.

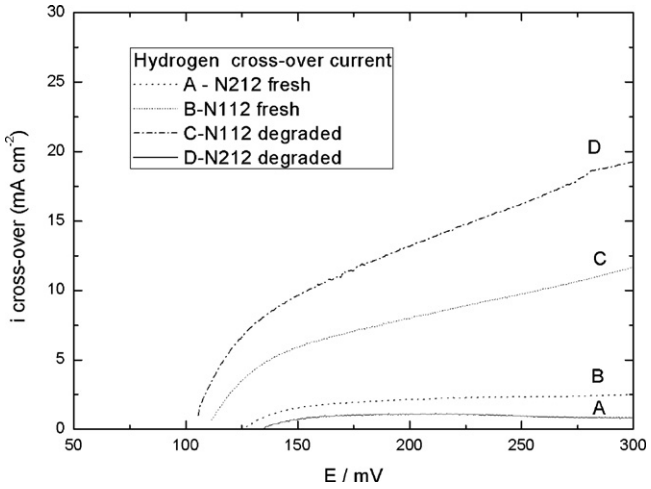

Fig. 10. Oxidation of the hydrogen crossing the fresh and degraded membranes. (A) N212, (B) N112 fresh membranes; (C) N112, (D) N 212 membranes after 24 h of degradation.

built with N212 presents better performance it may suffer larger performance degradation when compared to N112.

4. Conclusions

The results showed that Nafion N212 membrane displays higher performance than Nafion N112, when air is fed to the cathode of the PEMFC. However, the performance is the same when pure oxygen is employed. The maximum power density of the fuel cell is reached when the gases humidification are at the same temperature as that of the cell. The impedance and polarization results for the PEMFC working with different gas pressures and temperatures (cell and humidifiers), indicated that mass transport limitations, and ohmic drops have a strong influence in the fuel cell potentials. The polarization curves also showed some variations in the cell performance with the change of the Nafion load in the cathode catalyst layer, particularly at high current densities.

FTIR analyses showed that the chemical structure of Nafion does not change after accelerated degradation tests for both membranes. In spite of this, significant differences were observed in the morphology, mainly for N212. The electrochemical studies confirmed that the degradation of the membranes leads to a reduction in the fuel cell performance by increasing the H_2 crossover; the results also showed that the N212 membrane may be less durable than N112.

Acknowledgments

The authors thank the support of the Coordenação de Aperfeiçoamento de Pessoal de Nível Superior (CAPES), Conselho Nacional de Desenvolvimento Científico e Tecnológico (CNPq), and Fundação de Amparo a Pesquisa do Estado de São Paulo for their financial assistance.

References

[1] E. Antolini, J. Appl. Electrochem. 34 (2004) 563–576.
[2] M. Conte, A. Iacobazzi, M. Ronchetti, R. Vellone, J. Power Sources 100 (2001) 171–187.
[3] F. Jing, M. Hou, W. Shi, J. Fu, H. Yu, P. Ming, B. Yi, J. Power Sources 166 (2007) 172–176.
[4] S. Litster, G. McLean, J. Power Sources 130 (2004) 61–76.
[5] S. Maass, F. Finsterwalder, G. Frank, R. Hartmann, C. Merten, J. Power Sources 176 (2008) 444–451.
[6] V. Mehta, J.S. Cooper, J. Power Sources 114 (2003) 32–53.
[7] K. Scott, A.K. Shukla, Rev. Environ. Sci. Bio/Technology 3 (2004) 273–280.
[8] Y. Cai, J. Hu, H. Ma, B. Yi, H. Zhang, Electrochim. Acta 51 (2006) 6361–6366.
[9] G. Lin, W. He, T.V. Nguyen, J. Electrochem. Soc. 151 (2004) A1999–A2006.
[10] X. Liu, H. Guo, F. Ye, C.F. Ma, Electrochim. Acta 52 (2007) 3607–3614.
[11] T. Okada, J. Electroanal. Chem. 465 (1999) 1–17.
[12] P. Berg, K. Promislow, J.St. Pierre, J. Stumper, B. Wettonc, J. Electrochem. Soc. 151 (2004) A341–A353.
[13] Z. Qi, A. Kaufman, J. Power Sources 109 (2002) 38–46.
[14] N. Rajalakshmi, T.T. Jayanth, R. Thangamuthu, G. Sasikumar, P. Sridhar, K.S. Dhathathreyan, Int. J. Hydrogen Energy 29 (2004) 1009–1014.
[15] S. Ge, C.-Y. Wang, J. Electrochem. Soc. 154 (2007) B998–B1005.
[16] S. Litster, C.R. Buie, T. Fabian, J.K. Eaton, J.G. Santiago, J. Electrochem. Soc. 154 (2007) B1049–B1058.
[17] U. Pasaogullari, C.Y. Wang, J. Electrochem. Soc. 151 (2004) A399–A406.
[18] X. Ye, C.-Y. Wang, J. Electrochem. Soc. 154 (2007) B683–B686.
[19] Q. Yan, H. Toghiani, J. Wu, J. Power Sources 158 (2006) 316–325.
[20] V.A. Sethuraman, J.W. Weidner, A.T. Haug, L.V. Protsailob, J. Electrochem. Soc. 155 (2008) B119–B124.
[21] V.A. Paganin, E.A. Ticianelli, E.R. Gonzalez, J. Appl. Electrochem. 26 (1996) 297–304.
[22] C. Iojoiu, E. Guilminot, F. Maillard, M. Chatenet, J.-Y. Sanchez, E. Claude, E. Rossinot, J. Electrochem. Soc. 154 (2007) B1115–B1120.
[23] C. Chen, G. Levitin, D.W. Hess, T.F. Fuller, J. Power Sources 169 (2007) 288–295.
[24] E. Guilminot, A. Corcella, M. Chatenet, F. Maillard, F. Charlot, G. Berthomé, C. Iojoiu, J.-Y. Sanchez, E. Rossinot, E. Claude, J. Electrochem. Soc. 154 (2007) B1106–B1114.
[25] J. Healy, C. Hayden, T. Xie, K. Olson, R. Waldo, M. Brundage, H. Gasteiger, J. Abbott, Fuel Cells 5 (2005) 302–308.
[26] T. Kinumoto, M. Inaba, Y. Nakayama, K. Ogata, R. Umebayashi, A. Tasaka, Y. Iriyama, T. Abe, Z. Ogumi, J. Power Sources 158 (2006) 1222–1228.
[27] S. Kundu, M.W. Fowler, L.C. Simon, S. Grot, J. Power Sources 157 (2006) 650–656.
[28] S. Kundu, L.C. Simon, M.W. Fowler, Polym. Degrad. Stab. 93 (2008) 214–224.
[29] H. Tang, S. Peikang, S.P. Jiang, F. Wang, M. Pan, J. Power Sources 170 (2007) 85–92.
[30] V.O. Mittal, H. Russell Kunz, J.M. Fenton, J. Electrochem. Soc. 153 (2006) A1755–A1759.
[31] A. Bosnjakovic, S. Schlick, J. Phys. Chem. B 108 (2004) 4332–4337.
[32] A. Panchenko, H. Dilger, J. Kerres, M. Hein, A. Ullrich, T. Kaz, E. Roduner, Phys. Chem. Chem. Phys. 6 (2004) 2891–2894.
[33] B. Andreaus, G.G. Scherer, Solid State Ionics 168 (2004) 311–320.
[34] J. Zhang, B.A. Litteer, W. Gu, H. Liu, H.A. Gasteiger, J. Electrochem. Soc. 154 (2007) B1006–B1011.
[35] T.J.P. Freire, E.R. Gonzalez, J. Electroanal. Chem. 503 (2001) 57–68.
[36] V.A. Paganin, C.L.F. Oliveira, E.A. Ticianelli, T.E. Springer, E.R. Gonzalez, Electrochim. Acta 43 (1998) 3761–3766.
[37] R.R. Passos, E.A. Ticianelli, J. Braz. Chem. Soc. 13 (2002) 483–489.
[38] Y.W. Rho, O.A. Velev, S. Srinivasan, Y.T. Kho, J. Electrochem. Soc. 141 (1994) 2084–2089.
[39] T. Frey, M. Linardi, Electrochim. Acta 50 (2004) 99–105.
[40] E.A. Ticianelli, C.R. Derouin, S. Srinivasan, J. Electroanal. Chem. 251 (1988) 275–295.
[41] S.C. Roy, A.W. Harding, A.E. Russell, K.M. Thomas, J. Electrochem. Soc. 144 (1997) 2323–2328.
[42] R.R. Passos, V.A. Paganin, E.A. Ticianelli, Electrochim. Acta 51 (2006) 5239–5245.
[43] G. Sasikumar, J.W. Ihm, H. Ryu, Electrochim. Acta 50 (2004) 601–605.
[44] M. Inaba, T. Kinumoto, M. Kiriake, R. Umebayashi, A. Tasaka, Z. Ogume, Electrochim. Acta 51 (2006) 5746–5753.
[45] S. Kocha, P. Plasse, L. Onishi, D. Wheeler, J. Bett, Pre-Print Archive – American Institute of Chemical Engineers [Spring National Meeting], New Orleans, LA, United States, March 11–14, 2002.
[46] http://www.usfcc.com/resources/technicalproducts.html.